RSC Advances

ROYAL SOCIETY OF CHEMISTRY

www.rsc.org/advances

RSC Advances

RSCPublishing

ARTICLE

One-step facile fabrication of the sea urchin-like zirconium oxide for efficient phosphate sequestration

Cite this: DOI: 10.1039/x0xx00000x

Sufeng Wang[a], Mengxuan Ma[a], Wencang Man[a], Qingrui Zhang[a]*, Xiaolong Niu[a], Guiqing Sun[b], Wen Zhang[a] and Tifeng Jiao [a]*

Received 00th January 2014,
Accepted 00th January 2014

DOI: 10.1039/x0xx00000x

www.rsc.org/

Phosphate is a worldwide environmental issue, due to its possible cause of serious eutrophication and subsequently blue-green algae blooms. Sequestrating phosphate by exploitation of advanced materials with hierarchical morphology will be an important pathway. Herein, we fabricated a new sea urchin-like zirconium (IV) oxide (Ur-Zr) by one step facile alcoholysis solvothermal reaction for efficient phosphate removal. The as-obtained material exhibits a wide pH adsorption conditions with the optimal pH ranging from 1.0 to 6.0; competition results reveal that the Ur-Zr displays remarkable sorption selectivity for phosphate removal with coexisting of common anions (SO_4^{2-}, NO_3^- and Cl^- ions) at high concentrations, which can be ascribed to the unique hierarchical morphology and strong sorption affinity between Zr-O and phosphate species. Besides, the resultant Ur-Zr also shows a gradual sorption kinetic behavior, which can be well described by the pseudo-first-order model with the maximum sorption capacity of 74.8 mg/g. Additionally, the exhausted materials also process the recycled and repeated use properties by alkaline treatment. All the results demonstrate that the sea urchin-like zirconium (IV) oxide is a competent candidate for enhanced phosphate removal.

1. Introduction

Phosphate is an important nutritive substance in modern agriculture and industry, and the excessive presence of nitrogen and phosphorus in water bodies can bring about serious eutrophication and subsequently stimulate blue-green algae blooms. Recent 37 years' research demonstrates that reducing nitrogen inputs increasingly favor nitrogen-fixing cyanobacteria, while the extreme nitrogen limitation still remains highly eutrophic, due to the phosphate inputs[1]. To diminish eutrophication, the focus on decreasing inputs of phosphorus is required. Up to date, The World Health Organization (WHO) recommended a maximum phosphate discharge of 0.5-1.0 mg/L[2], and the rigorous regulation of 0.5mg/L limitation has been implemented in China for the new-built urban sewage treatment plant. In order to meet the strict standards, various technologies, including chemical precipitation, membrane, coagulation and adsorption[3], have been proposed for efficient sequestrating phosphate in waters. Among the available methods, adsorption technology might be an optimal choice and platform for reducing eutrophication.

To date, the traditional adsorbents, e.g. silica[4], biochar[5], carbon[6], zeolite[7] etc. always displayed inefficient phosphate sorption capability and lacking of applicability for enhancing phosphate removal, particular for the trace levels. In recent decade, nano-sized transition metal hydro (oxide) adsorbents have stimulated a wide research enthusiasm for phosphate removal and environmental remediation[8-10], owing to their strong inner-sphere complexation formation of metal-phosphate, size-dependent performances and environmental friendly properties[11]. Zirconium oxide (ZrO_2) is a promising inorganic functional material, which was widely used as catalyst[12], adsorbent[13], proton conductive membrane[14]. To yet, various methods have been explored to achieve the nanoscale fabrication for application improvements, e.g. solvothermal[15], chemical precipitation[16] and sol-gel procedure[17] for diverse nanorod[18], particle[19], nanowire[20,21] and fiber[22] formation. Particularly, as for the adsorbent for pollutant sequestration[23], the efficient adsorption performances are not merely dependent on the main chemical compositions or crystalline phase; the unique morphology and fine nanostructures will endow significant contributions[24]. Thus, achieving the specific morphology will be an important direction for efficient zirconium oxide fabrication.

Recently, Three-dimensional (3D) hierarchically layered nanostructure is constructed by the large micro-meter size building with nanoscale laminated sheets. The large micro-meter shapes can achieve the excellent separation / recycle features and mechanical strength; while the fine nano-laminated sheets will provide sufficient surface areas/activated sites for improving the adsorption performances[25-29]. Therefore, the new functional material with hierarchically nanostructure will be a desired option. Nevertheless,

the ZrO_2-based 3D hierarchically micro/nanostructure, e.g. flower like or sea urchin arrangement, is few reported, possibly ascribing to the high valence-states and different crystalline densities.

Herein, we successfully reported a new sea urchin-like zirconium oxide (denoted Ur-Zr) for phosphate sequestration. The unique structure is achieved by facile alcoholysis reaction in a solvothermal vessel, which needn't the additional complex ethylene glycol (EG) or poly (vinylpyrrolidone) (PVP) mediation as compared to the traditional solvothermal synthesise. The obtained unique needle-like structure can provide large surface areas and abundant activated sites for phosphate removal. More importance is the as-obtained Ur-Zr material also exhibits superior adsorption capacity (~ 74.8 mg/g), which can be well compared to the results from previous published literatures. Series batch sorption texts were also carried out to evaluate the phosphate sorption performance for reducing eutrophication.

2. Materials and methods

2.1 Preparation of the sea urchin-like zirconium oxide

All the chemicals are of analytical grade from Aladdin Reagent Station (Beijing, China). The urchin-like zirconium oxide was synthesized as the following: briefly, 3 g of zirconium oxychloride and 2 g of urea were dissolved in 50ml glycol solution (50% mass fraction) for completely mixing. The above mixtures were then poured into a teflon-lined autoclave for 8h reaction at 120 ^oC; after that, natural cooled to room temperatures, the resultant ZrO_2 precipitates were then reclaimed and washed by distilled water to removal the extra glycol solution. Finally, the white powders were desiccated successively at 60 ^oC for 24 h and 90 ^oC for 12 h in vacuum dry oven to obtain the desired sea urchin-like nano-ZrO_2 particles (Ur-Zr).

2.2 Batch phosphate adsorption tests

The phosphate uptake was well investigated by the conventional bottle-point methods[30]. To be specific, 0.05 g of Ur-Zr samples was introduced into a flask containing 50 ml phosphate solution at desired concentrations, solution pH values were adjusted using 1% HNO_3 or 1% NaOH, and the above bottles were then transferred into incubator shaker (SHZ-85, China) at preferred temperatures for 24 hours reaction to approach sorption equilibrium. Finally, the solutions were filtrated and the concentrations of phosphate and its corresponding solution pH were determined. Sorption competition evaluation was also conducted by similar methods. It is noteworthy that the common anions (SO_4^{2-}/NO_3^-/Cl^-) were also involved at different contents when necessary.

Kinetic experiments were carried out by introducing 0.2 g of Ur-Zr samples into a 1000 mL vessel with a known content of phosphate solution. The magnetic stirring was also assisted to ensure the homogeneous reaction. A 0.5 mL-solution was sampled at various time intervals and the kinetic data were obtained by determining the sampling phosphate concentrations versus the corresponding times.

Sorption-regeneration tests were also performed to assess the sorption stability, 0.05 g of Ur-Zr particles were used for adsorption test in a 50 mL solution containing known concentrations of phosphate as well as the common competing anions. Regeneration test was performed in the same vessel with 20 mL 5% NaOH solution as regenerant for 5h reaction. Note that, prior to the next cycles; the complete washing is necessary to remove extra alkaline solution for avoiding the possible influences on adsorption cycles.

2.3 Analysis and Characterization

The concentrations of phosphate samples were determined by the molybdenum blue spectrophotometric method. The sea urchin-like morphology of Ur-Zr was observed by SEM and TEM analysis. The urchin structure was recorded using a high-resolution transmission electron microscope (HRTEM), equipped with a Gatan CCD camera working at accelerating voltage of 200 kV; the corresponding morphology was taken on Hitachi S-4800 field emission scanning electron microscopy (FESEM) coupled with energy dispersive spectroscopy of the accelerating voltage of 5–20 kV. The X-ray diffraction (XRD) of the resultant Ur-Zr samples was achieved using an XTRA X-ray diffractometer (Switzerland) with Cu Kα radiation (λ = 1.5418 Å). N_2 sorption-desorption isotherm was performed for determining the pore structure parameters and surface areas using micrometrics ASAP 2020 (U.S.), the surface areas were calculated using the multipoint BET equation and the pore volumes were obtained using the Barrett–Joyner–Halenda (BJH) method

3. Results and discussion

3.1. Characterization of the sea urchin-like zirconium oxide

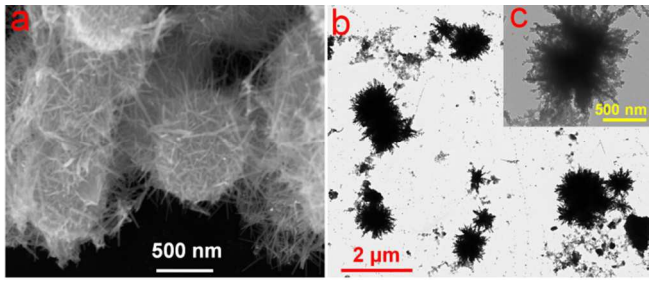

Fig. 1 The characteration of the sea urchin-like zirconium oxide (a) SEM image; (b) TEM image; (c) the magnification of the image b.

The morphology and structure of the prepared Ur-Zr was well characterized by SEM, TEM and XRD investigation. As depicted in Fig.1a, the as-obtained Ur-Zr material exhibits spherical shape with unique sea urchin structural morphology, further observation indicates that the formed structure is covered by many needle-like aggregates approximately 300-400 nm in length and 10-20 nm in width, such unique morphology indicates the potential large surface areas and efficient phosphate adsorption enhancement. Moreover, BET analysis (Table S1) further proves that the surface areas of the prepared Ur-Zr is approximately 64.5m^2/g.

TEM image of Fig 1b and Fig. S1 reveals that the formation of sea urchin sphere is a gradual process, the small size nanostructure

zirconium oxide (about 200 nm) tends to aggregate or grow into the large one (about 1-2 μm). Fig.1c further demonstrated that the ageing particles of Ur-Zr display a micro/nanometer structure. The particle size is approximately 1μm and the extended needle-like structure with size of 20-30 nm wide. This result coincides with the SEM investigation. Such unique morphology formation can be ascribed to the traditional "Ostwald ripening process", i.e. during the reaction process, a large number of nuclei are first formed in a short period of time through a well-known "Ostwald ripening process", followed by a slow crystal growth process. The aggregates continuously grow in size and density to form spheres with solid cores. Similar research has been observed and demonstrated in previous study[31-34]. XRD pattern (Figure S2) proved that the obtained Ur-Zr particles was highly crystalline samples, the major diffraction peaks belonged to the ZrO2 tetragonal phase, while minor diffraction peaks belonged to the ZrO2 monoclinic phase. Such results agreed with the previous study for tetragonal ZrO_2 fabrication[35,36] and the standard ZrO_2 spectrum.

3.2. Effects of solution pH on phosphate adsorption

The effects of solution pH on phosphate removal were conducted with the results of Fig. 2a. Observably, phosphate uptake onto Ur-Zr was a pH-dependent sorption process with the optimal pHs ranging from 1.0 to 6.0. Such powerful adsorption behaviors can be ascribed to the present species of zirconium oxide and sea urchin-like structure. As depicted in Fig. 2b, the zeta potential distribution reveals the obtained Ur-Zr samples display highly positive charges at acidic or neutral environments (pH_{zpc} = 6.4), thus the protonated Zr-OH_2^+ species will form in aqueous, which evidently can exert preferential adsorption toward negatively charged HPO_4^{2-}/$H_2PO_4^-$ species (Figure 2c).

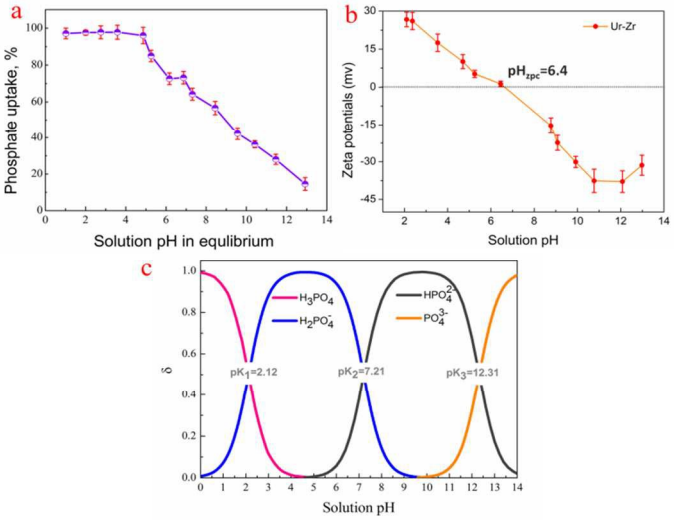

Fig. 2 (a) The solution pH effect onto Ur-Zr toward phosphate removal; (condition: dose 0.05g, 50mL solution containing 10mg/L phosphate at 298K) (b) the Zeta potential charge of Ur-Zr at various solution surroundings; (c) the phosphate species distributions at different solution pHs.

Moreover, the inspiring remarkable adsorption at strong acidic surroundings (pHs=1-2) was also detected, which is different from the conventional metal oxides for phosphate sequestration. Generally, at strong acidic conditions, the positively charged $H_2PO_4^-$ will tend to transform into the neutral H_3PO_4 species, which will exhibit unfavorable adsorption onto protonated zirconium oxide surfaces. Such efficient adsorption can be attributed to the urchin-like morphology with abundant activated sorption sites and the present strong inner-sphere complexation between Ur-Zr and phosphate species[13, 37], the possible reactions (Fig. 3) were presented as follows:

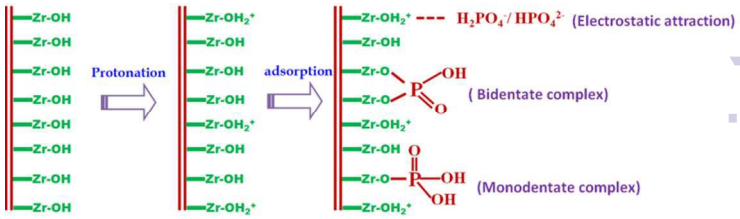

Fig. 3 Schematic diagram of possible phosphate adsorption reaction

Moreover, at alkaline surroundings, the decreasing adsorption can be ascribed to the deprotonated ZrO^- species formation, which will apply strong repulsion towards HPO_4^{2-} or PO_4^{3-} species. Besides, the strong competition from OH^- additions will also further restrain the phosphate uptake. It is noteworthy that the negligible adsorption at pH >13 further indicates the possible regeneration properties.

3.3. The present competition influences on phosphate removal

Case is known that the present common anions, including SO_4^{2-}, NO_3^- and Cl^- ions, are usually present in natural waters and industrial wastewaters at high concentrations. Therefore, it is required and necessary to estimate the sorption selectivity towards phosphate removal onto Ur-Zr and the commercial hybrid adsorbent FerriX^{TM} (Purolite, UK) was also involved for a reference. As is illustrated in Fig. 4, the referred FerriX^{TM} exhibits a gradual decrease and then steady sorption process with the common ion addition; the available phosphate removal efficiency is approximately 42%-48%. Considering the chemical composition of quaternary ammonium (-$CH_2N(CH_3)_3Cl$) and ferric oxides onto FerriX^{TM}, it is believed that the modified ammonium groups will exert phosphate removal by non-specific electrostatic adsorption, and the encapsulated ferric oxides can be assigned to the stabilized strong phosphate uptake by Fe-O-P bonds formation. Comparatively, the as-obtained Ur-Zr displays satisfactory phosphate sorption performances. The slightly influences on common anion additions and distinguished sorption efficiency of above 95% further proved the remarkable selectivity and promising applicability toward phosphate sequestration.

To further elucidate the potential sorption selectivity onto Ur-Zr material. The distribution ratio K_d (L/g) was determined by the following equation and the results are presented in Table S2.

$$K_d = \frac{(C_0 - C_e)}{C_e}\frac{V}{m} \quad (1)$$

Where C_0 (mg/L) is the initial phosphate concentrations of the solution, V (L) represents the volume of the solution, and m (g) is the mass of the adsorbent. Evidently, the remarkable larger K_d values than the commercial FerriX^{TM} further verify its preferential sorption performances.

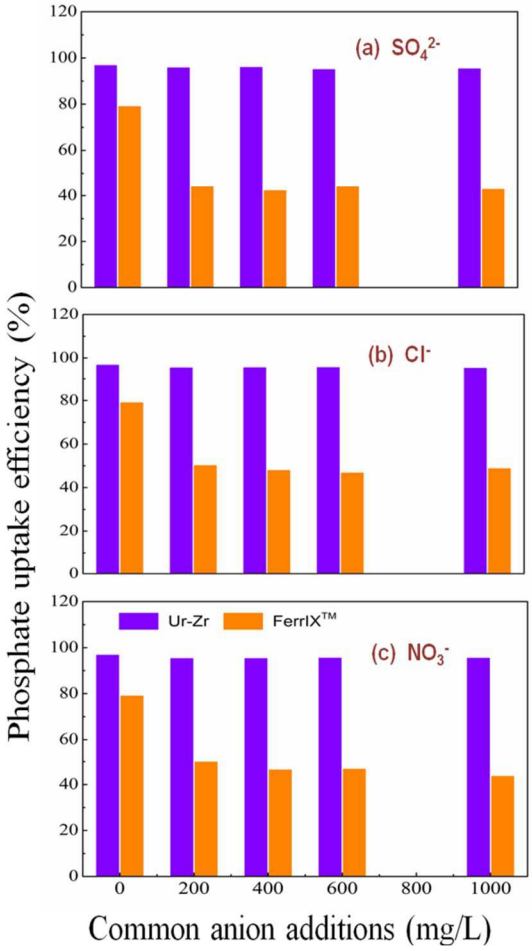

Fig. 4 Effect of the competing anion on phosphate uptake by Ur-Zr and the commercial FerriX^{TM} at 298 K. The adsorbent dose was 1.0 g/L with 10.0 mg /L of phosphate ions.

To further elucidate the possible selective adsorption mechanism, the XPS investigation (Fig. 5) was also performed to gain some new insights into the phosphate uptake process. The presence of distinct peak at ~133.5 eV after phosphate uptake onto Ur-Zr suggests the successful phosphate intercalation, while the standard P 2p spectrum from the purified KH_2PO_4 appears at ~134.0 eV (Fig. 5b). the significant ~0.5 eV binding energy shifts to a lower energy level indicate the present strong affinity between phosphate and the prepared Ur-Zr. Moreover, the Zr 3d spectrum was displayed at Figure 6c, the prominent peaks from $Zr3d_{3/2}$ and $Zr3d_{5/2}$ were located at ~183.5 eV and ~181.3 eV, respectively, while after phosphate uptake, the originated Zr 3d peaks are significant weaken and two new peaks appear at ~184.3 eV and ~182.1 eV respectively (Fig. 5d). The new emerged peaks might be ascribed to form the new phosphate- zirconium complex substance and the corresponding large binding energy shifts of 0.8 eV indicates the presences of powerful affinity of Zr and phosphate species and favorable adsorption.

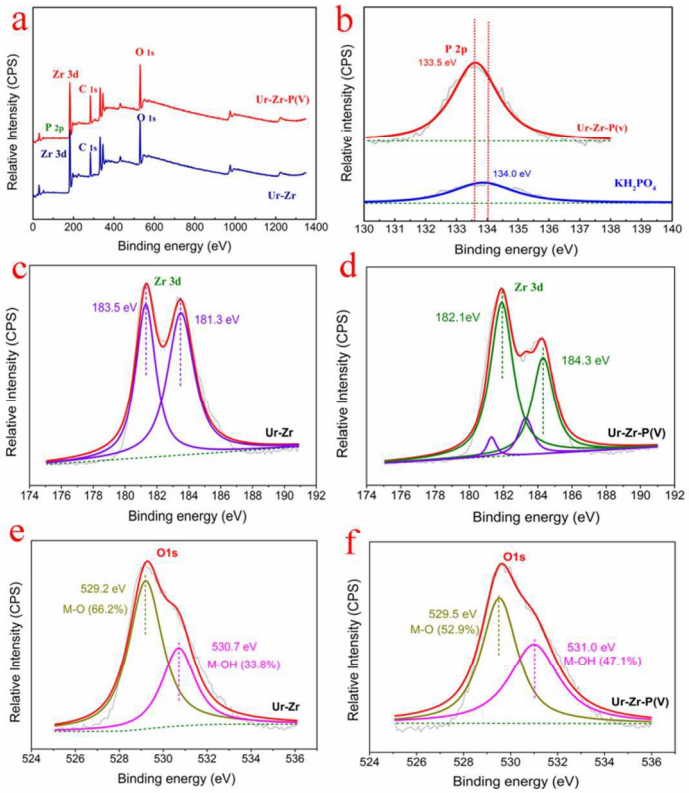

Fig. 5 The XPS spectra analysis. (a) the XPS survey of the Ur-Zr and phosphate loaded Ur-Zr; (b) the comparisons of P 2p peaks onto phosphate loaded Ur-Zr samples and purified $K_2H_2PO_4$; (c) Zr 3d spectrum onto the bared Ur-Zr; (d) Zr 3d spectrum onto phosphate loaded Ur-Zr samples; (e) O1s analysis onto Ur-Zr; (f) O 1s variations onto phosphate loaded Ur-Zr samples.

Additionally , the variation of O 2p binding energy of the prepared Ur-Zr samples (Fig. 5e-f). Based on the different oxygen species, the O 1s spectra are separated into two peaks of M-O (~529.2 eV) and M-OH(~530.7 eV). As for the primitive Ur-Zr, the area fractions of M-O and M-OH are occupied approximately~66.2% and ~33.8% respectively. Whereas, the phosphate uptake can lead to an obvious increases on M-OH species (~47.1%) and binding energy shifts of ~0.3 eV, which implies the possibly preferential adsorption. In theory, the phosphate adsorption can evoke the replace of M-OH species by formation of M-O-P bonds, Considering the possible hydroxyl contributions from one or two P-OH groups by different H_2PO_4/HPO_4 species, it is believed that zirconium hydroxyl sites are capable of exerting robust interaction with target phosphates spontaneously.

3.4. Sorption kinetics and isotherms

Sorption kinetic tests were conducted and the results were shown in Fig. 6a. It can be seen that phosphate uptake exhibits a continuous

adsorption process, with the equilibrium times of approximately 250 min. such gradual adsorption can be ascribed to the sea urchin-like structure. i.e. the diffusion of phosphate onto Ur-Zr samples is a plodding adsorption, at the initial beginning stage, the phosphate uptake is dominated by the surface and needle-like structure, and further increasing contact time will bring about the inner pore/surface diffusion into the sea urchin Ur-Zr for approaching sorption equilibrium.

To further elucidate the adsorption process, the classic adsorption models for kinetic evaluation were performed and the relevant equations as follows[38,39]:

The pseudo-first-order model:

$$\log(q_e - q_t) = \log q_e - \frac{k}{2.303}t \quad (2)$$

The pseudo-second-order model:

$$\frac{t}{q_t} = \frac{1}{k\,q_e^{\,2}} + \frac{t}{q_e} \quad (3)$$

The intraparticle diffusion model

$$q_t = k_p * t^{0.5} + C \quad (4)$$

Where q_t and q_e represent the amount of phosphate adsorbed (mg/g) in equilibrium and time t respectively, and k or k_p values are the kinetic rate constant. The detailed fitting parameters of the models were shown in TableS3. Evidently, the kinetic data can be well described by pseudo-first-order model with the high correlation coefficient (R^2>0.987). Additionally, the well fitted intraparticle diffusion model (Fig. 6b, R^2>0.990) further proves that the phosphate adsorption onto Ur-Zr is dominated by the inner pore diffusion process.

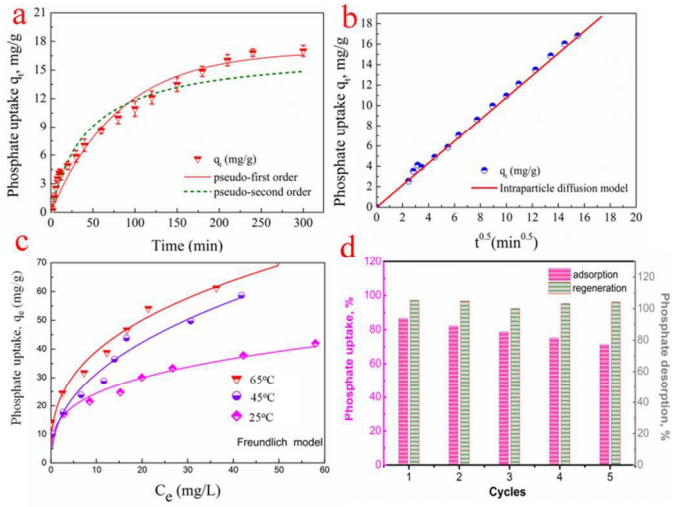

Fig. 6 (a) sorption kinetic curves by pseudo-first/second order fittings; (b) intraparticle diffusion model fittings for kinetic data; (c) adsorption isotherms at different temperatures; (d) sorption- regeneration tests (adsorption conditions: 0.5g/L, initial phosphate 10mg/L at 298K, NO_3^-=SO_4^{2-}=Cl^- =200mg/L, pH =5.8-6.2; regeneration: 5% NaOH solution at 298K).

Adsorption isotherms (Figure 6c) reveal that phosphate uptake is a temperature-relevant endothermic process and the high temperatures will favor for phosphate sequestration. Additionally, the representative models, i.e. Langmuir, Freundlich and Temkin, were also conducted to describe sorption process with the following equations

Langmuir model

$$Q_e = \frac{Q_{max} k_L C_e}{1 + k_L C_e} \quad (5)$$

Freundlich model (6)

$$Q_e = k_F C_e^{\,1/n}$$

Temkin model

$$Q_e = \frac{RT}{b}\ln(AC_e) \quad (7)$$

Where C_e represents the concentrations of phosphate at equilibrium and Q_e is assigned to the corresponding adsorption capacity; Q_{max} is the maximum phosphate capacity per gram, and k_L k_F and n as well as the A and b of Temkin constants to be determined. The detailed fitting results were shown in Table S4, the larger R^2 values suggest that the sorption process can be well described by the Freundlich models reasonably and the maximum sorption capacity is approximately 74.8 mg/g, which can be well compared with the performances in published literatures (Table 1)

Table 1 The phosphate sorption capacity comparison in published literatures

Adsorbent	Q_{max} (mg/g)	Optimal pH	Temperature	References
Granular ferric hydroxide	1.6	6.5-7.5	298K	40
Modified chitosan beads	60.6	1.0-3.5	298K	41
Mg-Al hydrotalcite-loaded kaolin clay	11.92	2.5-9.5	298K	42
Pyromellitic acid intercalated ZnAl - LDHs	41.45	7.0	303K	43
Cerium - zirconium binary oxide nanoadsorbents	112.23	2.0-6.0	298K	44
Modified Iron Oxide-based Sorbents	38.8	7.0	298K	45
Cu(II) - loaded polyethersulfone-type metal affinity membrane	74.0	4.0-7.0	293K	46
Mesoporous silica spheres loaded with lanthanum	42.76	3.0-6.0	298K	47
Zirconium(IV) loaded cross - linked chitosan particles	71.68	3.0	303K	48
La-modified tourmaline	108.7	7.0	298K	49
Sea urchin-like ZrO_2	**74.8**	**1.0-6.0**	**298K**	**This work**

3.5. Sorption-regeneration cycles

To estimate the sorption stability of the prepared Ur-Zr material, sorption-regeneration tests were conducted and the results were depicted in Figure 6d. The results indicate that the sea urchin structural Ur-Zr is an effective and recyclable adsorbent for phosphate removal using 5% NaOH solution as regenerants. The slight capacitys lose for five cycles might be partly ascribed to the possible irreversible sites and morphology variations by alkaline treatments.

4. Conclusions

In the present study, we successfully prepared a new sea urchin-like zirconium oxide by one step facile alcoholysis solvothermal reaction for efficient phosphate removal. The unique hierarchically structural and strong sorption affinities grant a wide pH sorption range, fast kinetics, remarkable sorption selectivity and comparative phosphate sorption capacity. Additionally, the exhausted material also processes the recycle and repeated use properties by alkaline treatment. This work provides a new approach for high valence hierarchically structural metal oxide synthesis and its potential distinguished environmental application.

Acknowledgements

We greatly acknowledge the financial support from the National Natural Science Foundation of China (Grant Nos. 40830746 and 41271102, 21207112, 21473153 and 51578476), the National Science Technology Support Program (Grant No. 2011BAD13B06), Natural Science Foundation of Hebei Province of China (Grant Nos. 2014203207), and Key Laboratory of Reservoir Aquatic Environment, Chongqing Institute of Green and Intelligent Technology, Chinese Academy of Science (Grant No. RAE2014CE03B).

Notes and references

[a] Hebei Key Laboratory of Applied Chemistry, School of Environmental and Chemical Engineering, Yanshan University, Qinhuangdao 066004, PR China
[b] Hebei Ocean & Fisheries Science Research Institute, Qinhuangdao 066200, PR China

1. D. W. Schindler, R. Hecky, D. Findlay, M. Stainton, B. Parker, M. Paterson, K. Beaty, M. Lyng and S. Kasian, *Proc. Natl. Acad.Sci. USA*, 2008, **105**, 11254-11258.
2. W. H. Organization, *Guidelines for drinking-water quality: recommendations*, World Health Organization, 2004.
3. T. Almeelbi and A. Bezbaruah, *J. Nanopart. Res.*, 2012, **14**, 1-14.
4. Y. Yu, R. Wu and M. Clark, *J. Colloid Interface Sci.*, 2010, **350**, 538-543.
5. Y. Yao, B. Gao, J. Chen, M. Zhang, M. Inyang, Y. Li, A. Alva and L. Yang, *Bioresource Technol.*, 2013, **138**, 8-13.
6. L. Zhang, L. Wan, N. Chang, J. Liu, C. Duan, Q. Zhou, X. Li and X. Wang, *J. Hazard. Mater.*, 2011, **190**, 848-855.
7. J. Chen, H. Kong, D. Wu, Z. Hu, Z. Wang and Y. Wang, *J. Colloid Interface Sci.*, 2006, **300**, 491-497.
8. P. Z. Ray and H. J. Shipley, *RSC Adv.*, 2015, **5**, 29885-29907.
9. M. Hua, S. Zhang, B. Pan, W. Zhang, L. Lv and Q. Zhang, *J. Hazard. Mater.*, 2012, **211**, 317-331.
10. P. Xu, G. M. Zeng, D. L. Huang, C. L. Feng, S. Hu, M. H. Zhao, C. Lai, Z. Wei, C. Huang and G. X. Xie, *Sci. Total. Environ.*, 2012, **424**, 1-10.
11. D. G. Strawn and D. L. Sparks, *J. Colloid Interface Sci.*, 1999, **216**, 257-269.
12. A. M. Hengne and C. V. Rode, *Green Chem.*, 2012, **14**, 1064-1072.
13. Y. Su, H. Cui, Q. Li, S. Gao and J. K. Shang, *Water Res.*, 2013, **47**, 5018-5026.
14. G. Nawn, G. Pace, S. Lavina, K. Vezzù, E. Negro, F. Bertasi, S. Polizzi and V. Di Noto, *ChemSusChem*, 2015, **8**, 1381-1393.
15. G. Li, Z. Hong, H. Yang and D. Li, *J. Alloy. Compd.*, 2012, **532**, 98-101.
16. C. Huang, Z. Tang and Z. Zhang, *J. Am. Ceram. Soc.*, 2001, **84**, 1637-1638.
17. Q. Mahmood, A. Afzal, H. M. Siddiqi and A. Habib, *J. Sol-gel. Sci. Technol.*, 2013, **67**, 670-674.
18. Y. Liu, C. Zheng, W. Wang, Y. Zhan and G. H. Wang, *J. Am. Ceram. Soc.*, 2002, **85**, 3120-3122.
19. T. S. Sreeremya, A. Krishnan, L. N. Satapathy and S. Ghosh, *RSC Adv.*, 2014, **4**, 28020-28028.
20. W.-S. Dong, F.-Q. Lin, C.-L. Liu and M.-Y. Li, *J. Colloid Interface Sci.*, 2009, **333**, 734-740.
21. B. Xu and X. Wang, *Dalton. Trans.*, 2012, **41**, 4719-4725.
22. M. Biswas and S. Bandyopadhyay, *Mater. Lett.*, 2013, **101**, 13-16.
23. L. A. Rodrigues, L. J. Maschio, L. d. S. Cividanes Coppio, G. P. Thim and M. L. Caetano Pinto da Silva, *Environ. Technol.*, 2012, **33**, 1345-1351.
24. Z. Shu, X. Jiao and D. Chen, *CrystEngComm*, 2012, **14**, 1122-1127.
25. C. Cao, J. Qu, F. Wei, H. Liu and W. Song, *Acs Appl. Mater. Interfaces*, 2012, **4**, 4283-4287.
26. E.-J. Kim, C.-S. Lee, Y.-Y. Chang and Y.-S. Chang, *Acs Appl. Mater. Interfaces*, 2013, **5**, 9628-9634.
27. H. Wang, Q. Liang, W. Wang, Y. An, J. Li and L. Guo, *Cryst. Growth Des.*, 2011, **11**, 2942-2947.
28. W. Li, Y. Bu, H. Jin, J. Wang, W. Zhang, S. Wang and J. Wang, *Energ. Fuel*, 2013, DOI: 10.1021/ef401190b.
29. F. Wang, H. Dai, J. Deng, G. Bai, K. Ji and Y. Liu, *Environ. Sci. Technol.*, 2012, **46**, 4034-4041.
30. Q. Zhang, Q. Du, M. Hua, T. Jiao, F. Gao and B. Pan, *Environ. Sci. Technol.*, 2013, **47**, 6536-6544.
31. W. Ostwald, Z. Phys. Chem., 1900, 34, 495–503.
32. S. J. Bao, Q. L. Bao, C. M. Li, T. P. Chen, C. Q. Sun, Z. L. Dong, Y. Gan and J. Zhang, *Small*, 2007, 3, 1174–1177.
33. B. Li, G. Rong, Y. Xie, L. Huang and C. Feng, *Inorg. Chem*., 2006, 45, 6404–6410.
34. W. Wang, T.F. Jiao, Q.R. Zhang, X.N. Luo, J. Hu, Y. Chen, Q.M. Peng, X.H. Yan and B.B. Li *RSC Adv.*, 2015, **5**, 56279-56285.
35. H. Cui, Y. Su, Q. Li, S. Gao, and J.K. Shang, *Water Res.*, 2013, 47, 6258-6268.
36. V. G. Deshmane and Y. G. Adewuyi, *Micro. Meso. Mater.*, 2012, 148, 88-100.
37. J. Lǔ, H. Liu, R. Liu, X. Zhao, L. Sun and J. Qu, *Powder Technol.*, 2013, **233**, 146-154.
38. H. Qiu, L. Lv, B.C. Pan, Q.J Zhang, W.M. Zhang and Q.X. Zhang, *J. Zhejiang Univ. Sci. A*, 2009, **10**, 716-724.

39. Z.W. Xu, L. Cheng, J. Shi, J.G. Lu, W.M. Zhang, Y.L. Zhao, F.Y. LI, M.D. Chen, *Environ. Sci. Pollut. Res*. 2014, 21, 6574-6577.
40. M. Kartashevsky, R. Semiat, C.G. Dosoretz, *Desalination*, 2015, 364, 53–61.
41. X. Liu, L. Zhang, *Powder Technol*., 2015, 277,112–119.
42. L. Deng, Z. Shi , *J. Alloy.Compd.* , 2015, 637, 188–196.
43. Q. Q. Yu, Y. Q. Zheng, Y. P. Wang , L. Shen, H.T. Wang,Y.M. Zheng, N. He, Q.B. Li, *Chem. Eng. J.*, 2015, 260, 809–817.
44. Y. Su, W. Y. Yang, W. Z. Sun, Q. Li, J. K. Shang, *Chem. Eng. J.*, 2015, 268,270–279.
45. J.Lalley, C. Han, X. Li, D. D. Dionysiou, M. N. Nadagouda, *Chem. Eng. J.*, 2016, inpress doi: 10.1016/j.cej.2015.08.114
46. L.Z. Song, , J. B. Huo, X. L. Wang, F. F. Yang, J. He, C. Y. Li, *Chem. Eng. J.*, 2016, 284,182–193.
47. W. Huang, X. Yu, J. Tang, Y. Zhu, Y. Zhang, D. Li, *Micro. Meso. Mater.* 2015, 217, 225-232.
48. Q. Liu, P. Hu, J. Wang, L. Zhang, R. Huang, *J. Taiwan Inst. Chem. E.* 2015, in press doi:10.1016/j.jtice.2015.08.012.
49. G. Li, D. Chen, W. Zhao, X. Zhang, *J. Environ.Chem. Eng*., 2015, 3, 515-522.

Graphical Abstract

Phosphate is a worldwide environmental issue, due to the possible cause of serious eutrophication. Herein, we fabricated a new sea urchin-like zirconium (IV) oxide by one step facile alcoholysis solvothermal reaction, which exhibits efficient phosphate sequestration with the remarkable selectivity, large capacity and recycled use properties.